Trego_Figure S1

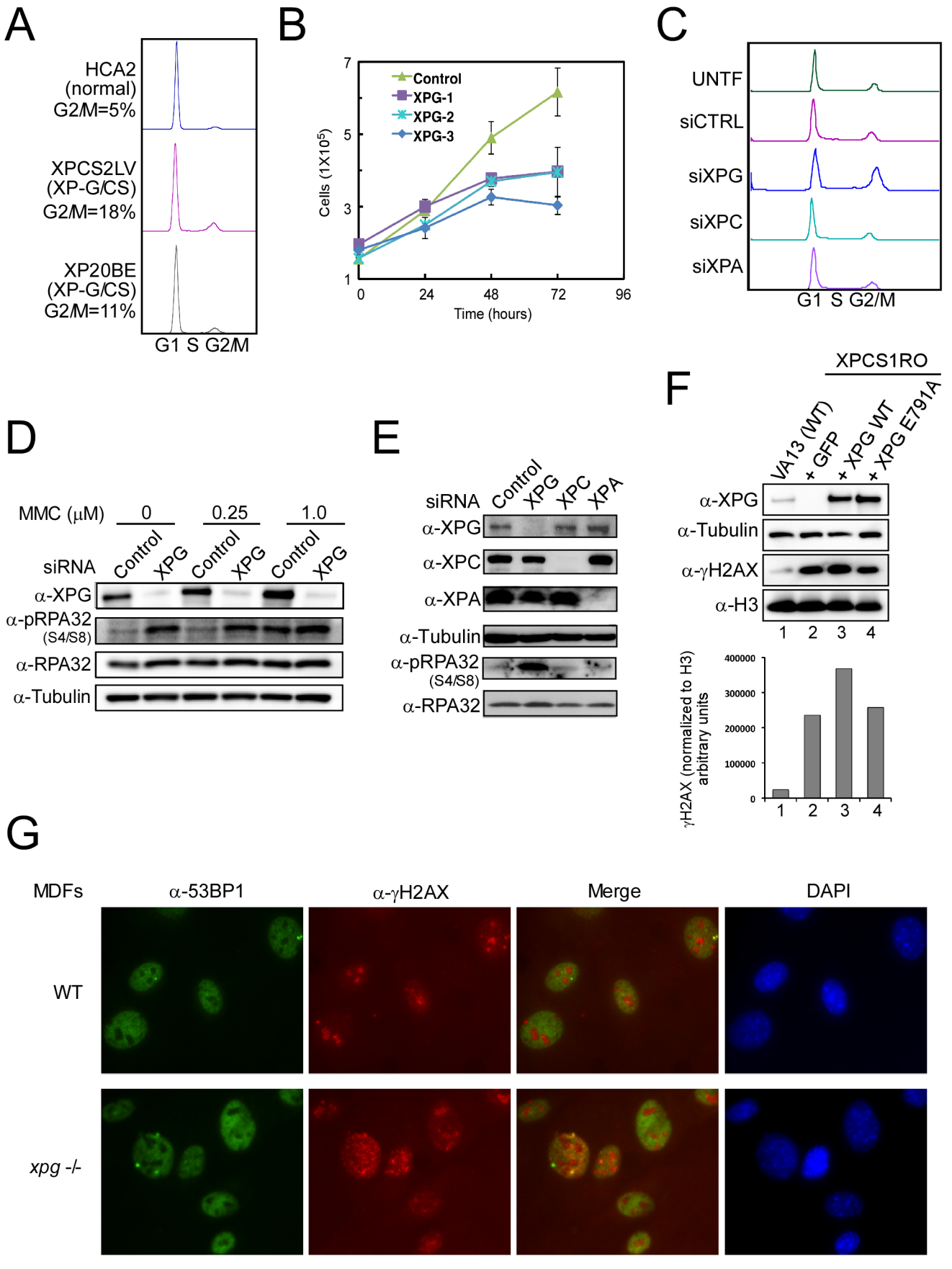

Trego_Figure S2

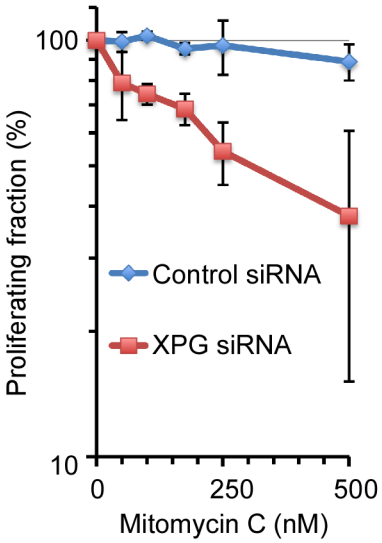

Trego_Figure S3

A

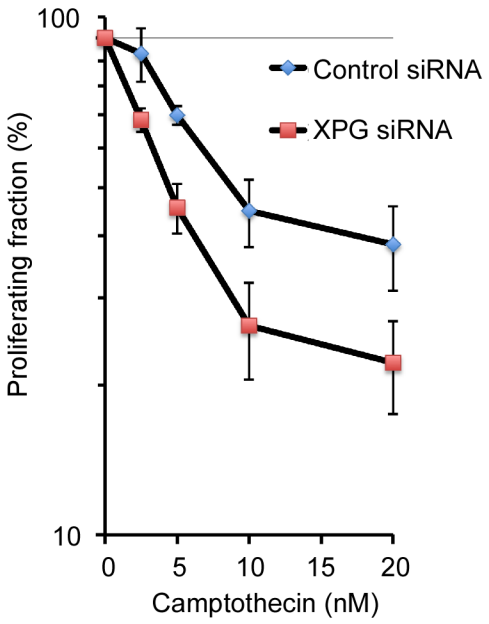

B

C

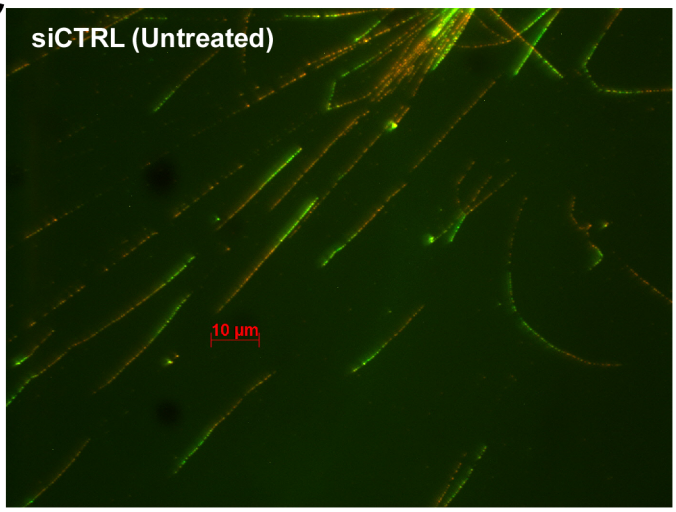

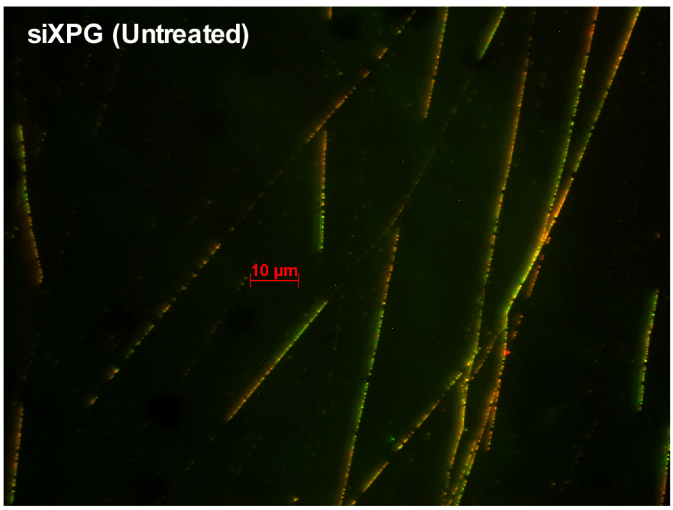

Trego_Figure S4

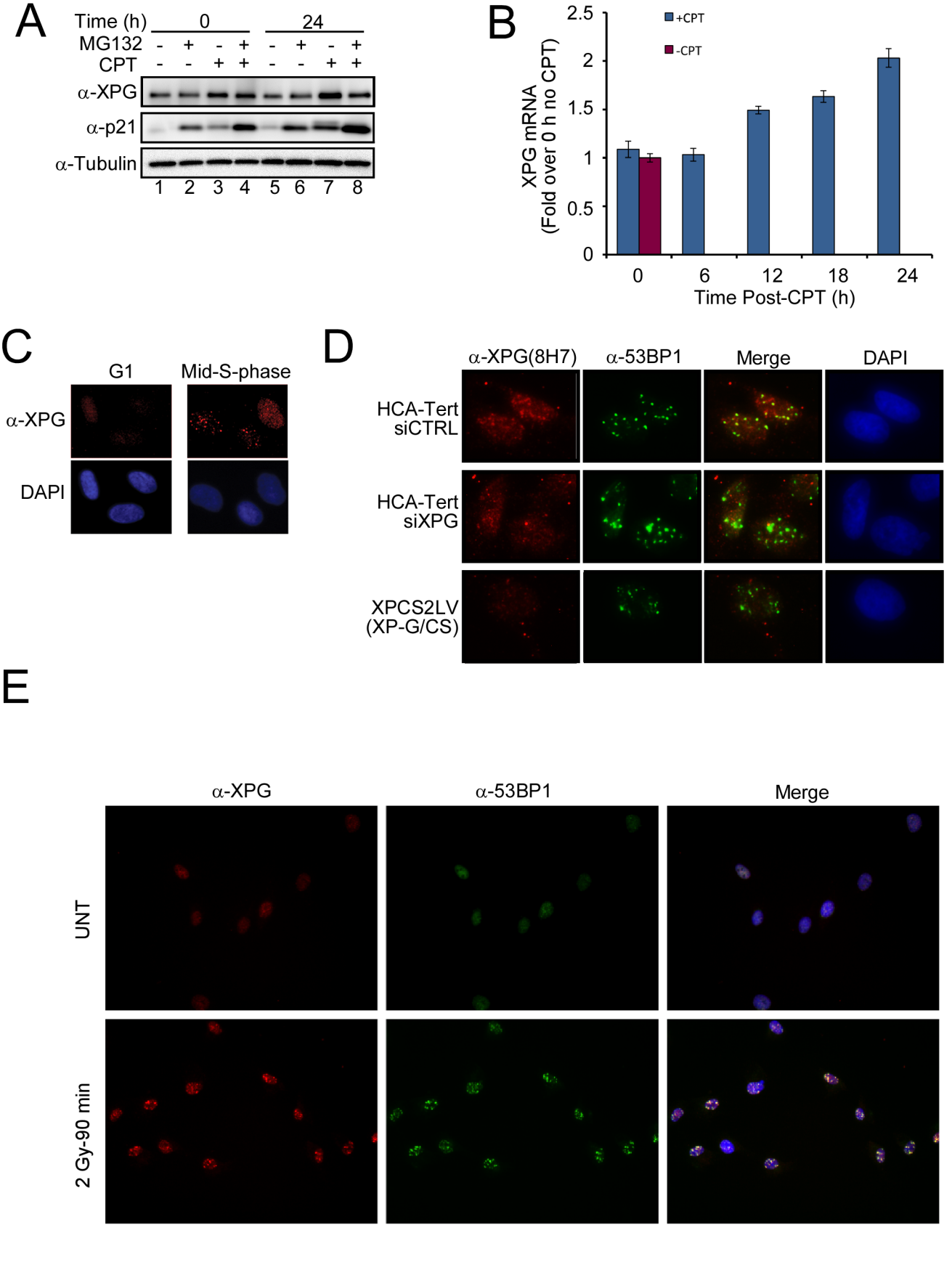

Trego_Figure S5

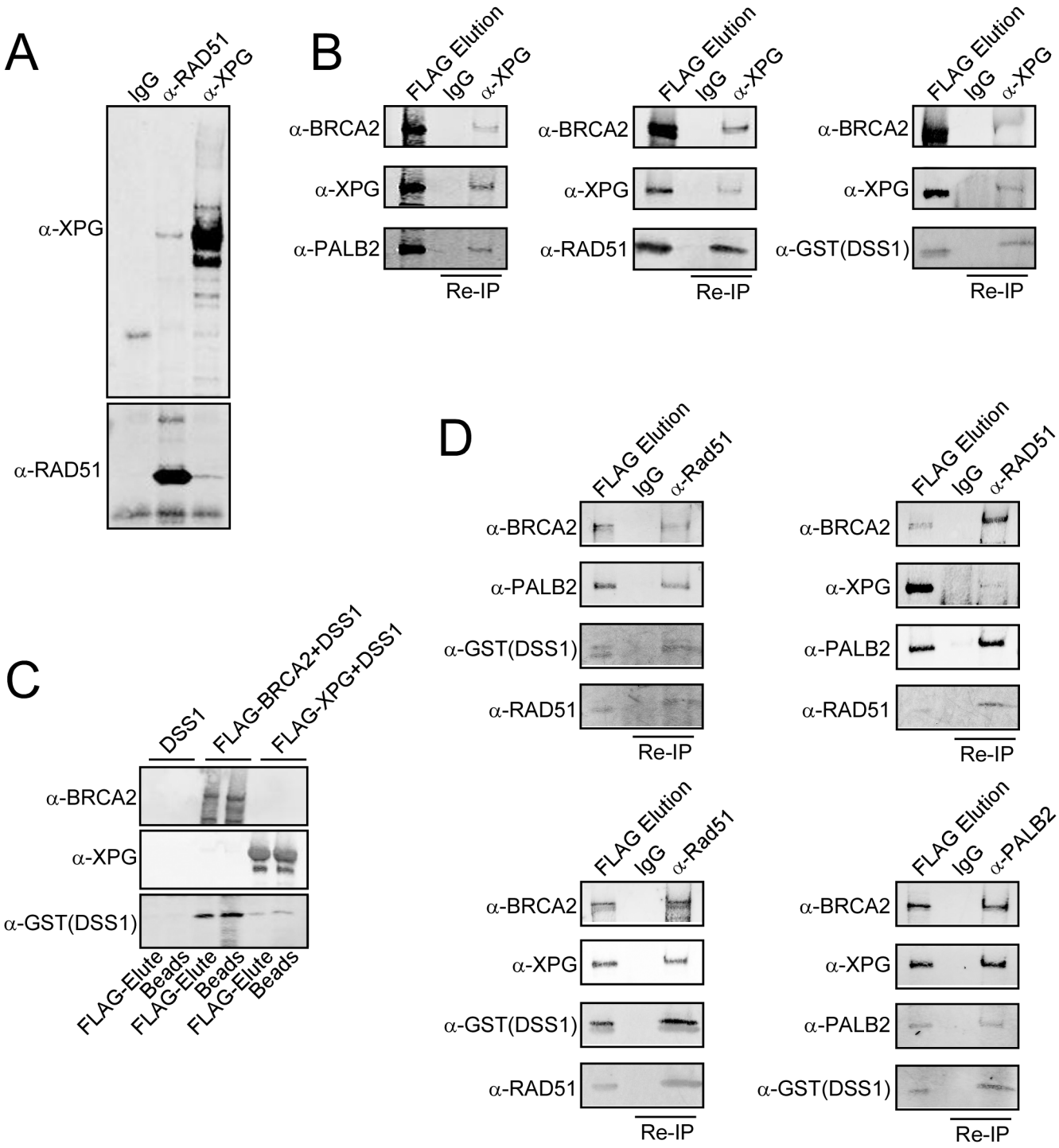

Trego_Figure S6

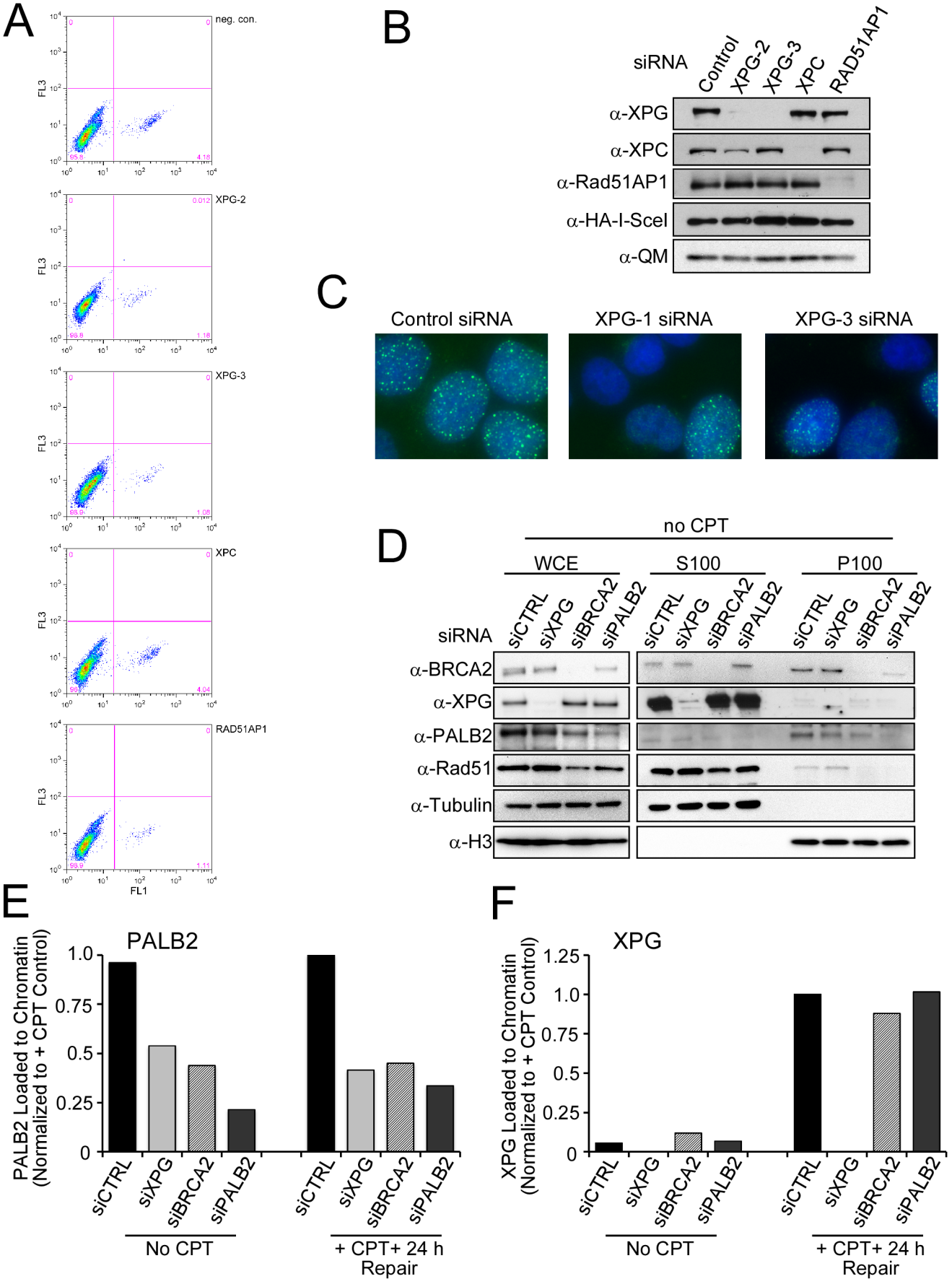

Trego_Figure S7

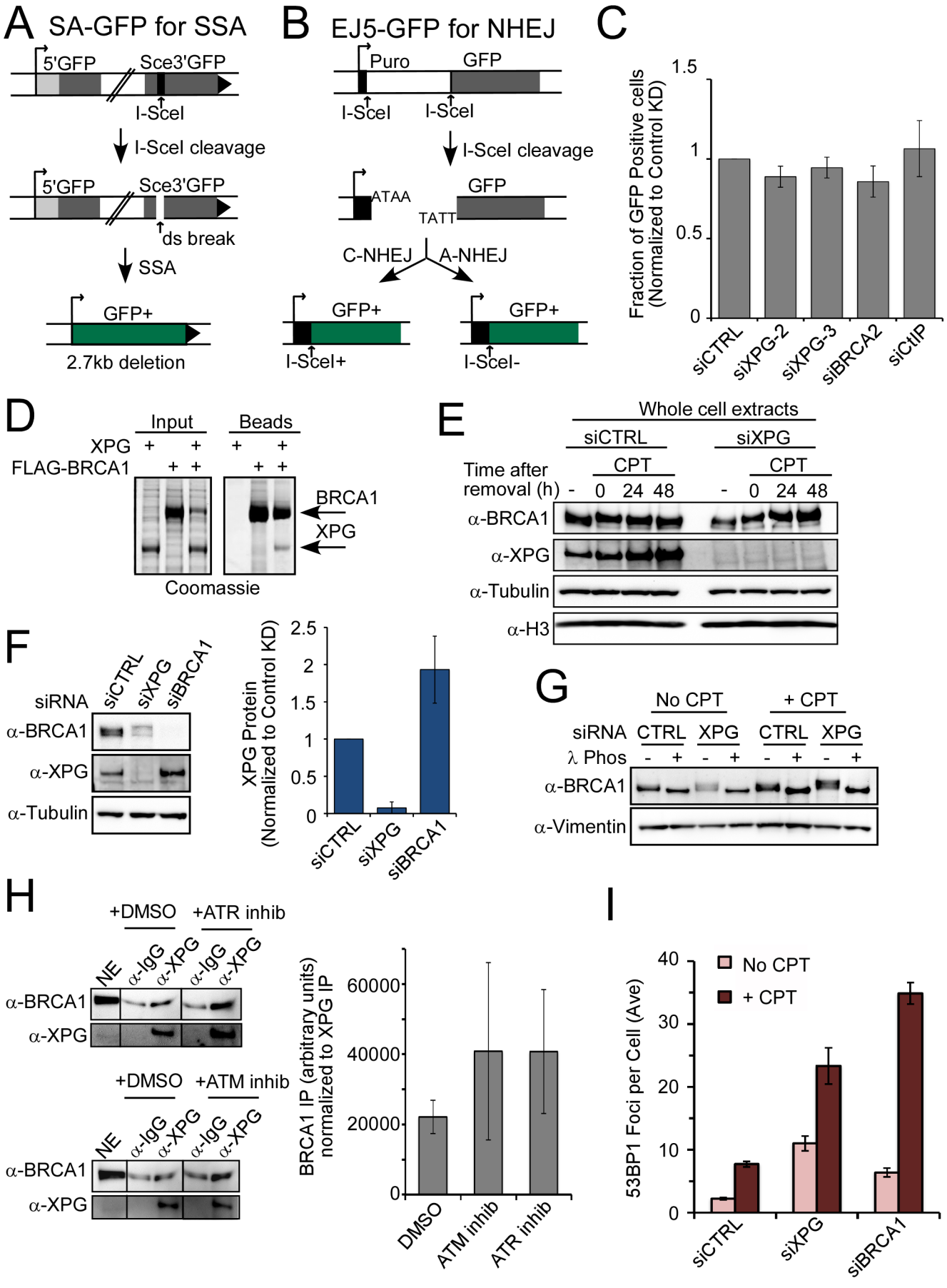

SUPPLEMENTAL INFORMATION

Figure legends

Figure S1: Loss of XPG causes spontaneous DNA damage independent from defective NER; related to Figure 1.

(A) XP-G/CS cells have an increased G2 population. The cell cycle distribution of primary fibroblasts, HCA2 (WT), or 2LV (XP-G/CS) or XP20BE (XP-G/CS) cells was determined by FACS analysis of propidium iodide stained cells. Plots were analyzed using FlowJo and Watson (Pragmatic) analysis.

(B) Cell growth is reduced in XPG-depleted cells. U2OS transfected with the indicated siRNAs were monitored for proliferation beginning 24 hours after the second transfection.

(C) Effect of XPG, XPA, or XPC depletion on cell-cycle progression in U2OS cells. G1, S, and G2/M phases were determined by flow cytometry using propidium iodide staining and were analyzed using FlowJo and Watson (Pragmatic) analysis.

(D) The amount of pRPA32 in XPG KD cells is roughly equivalent to that after treatment of control KD cells with 1 μM MMC. Extracts from HeLa cells transfected with control or XPG siRNAs were harvested 24 hours after mock or MMC treatment (250 nM or 1 μM for 1 h).

(E) pRPA32 is elevated in XPG-depleted cells, but not in those depleted for XPC or XPA. Western blot analysis of total extracts from U2OS cells transfected with the indicated siRNAs targeting XPG, XPC, XPA, or control siRNA.

(F) γH2AX is elevated in the SV40-transformed XP-G/CS cell line XPCS1RO (lane 2 vs lane 1). The effect is not complemented by addition of either WT-XPG (lane 3) or endonuclease-dead XPG (XPG mutant E791A; lane 4) (Staresincic et al., 2009). Western blot analysis of total extracts from VA13 cells or XPCS1RO cells stably transfected with either plasmids expressing GFP, WT-XPG-HA, or XPG-E791A-HA. Quantification of γH2AX protein amount was normalized to Histone H3 and plotted for each cell line.

(G) Primary mouse dermal fibroblasts (MDFs) from littermates, either WT or knocked out for XPG (*xpg* -/-) (Barnhoorn et al., 2014). Cells were immunostained using rabbit anti-53BP1 (green) and mouse anti-

γH2AX antibodies (red). The merged images for foci overlap (yellow), and DAPI (blue) stained nuclei are shown. Note: The spots in both wt and KO MDFs that stain intensely for γH2AX but not 53BP1 are DAPI-bright heterochromatic regions.

Figure S2. XPG is required for genome stability and cell survival; related to Figure 2

XPG-depleted cells are sensitive to MMC. Control- and XPG-depleted hTERT immortalized normal human fibroblasts (HCA2-hTERT) were assayed for ability to replicate after the damaging treatment (as a surrogate assay for survival) by BrdU incorporation following MMC treatment. Data represent the mean ± SD for N=3.

Figure S3: XPG mediates recovery from replication stress; related to Figure 3.

(A) XPG-depleted cells are sensitive to camptothecin (CPT). Control- and XPG-depleted hTERT immortalized normal human fibroblasts (HCA2-hTERT) were assayed for cellular sensitivity to CPT damage by ability to replicate following treatment, as measured by BrdU incorporation. Data represent the mean ± SD for N=3.

(B) Diagram of the protocol used for the DNA fiber analysis experiments, showing the addition of nucleotide analog CldU (red) for 45 min followed by washing and addition of IdU (green) for 45 min prior to processing for the DNA fiber assay.

(C) Representative micrographs of DNA fibers from undamaged U2OS cells transfected with control siRNA (top) or XPG siRNA (bottom) following the protocol described in (B).

Figure S4. XPG accumulates at sites of DNA double-strand breaks; related to Figure 4.

(A) Western blot analysis of U2OS cells treated with DMSO (- CPT) or 20 nM CPT for 24 hours, and then washed and harvested either immediately, or after 24 h repair. Where indicated, cells were treated with MG132 (2 μM) 16 h before harvest to inhibit proteasomal degradation. p21 was used as a positive control for proteasome inhibition, since MG132 inhibits p53 degradation, leading to p21 upregulation (Mazroui et al., 2007).

(B) *XPG* mRNA is upregulated following CPT treatment as early as 12 h post CPT removal. The expression of *XPG* mRNA was measured using qRT-PCR. Data represent the mean ± SD for N=3.
(C) XPG foci do not form during G1 phase, but during S-phase. hTERT immortalized HCA2 cells were synchronized into G1 phase or into mid-S-phase (Davalos and Campisi, 2003), and stained for XPG foci (red).
(D) XPG foci overlap with 53BP1 (a marker of DSBs) after IR. hTERT immortalized HCA2 cells transfected with control siRNA (top panel) or siRNA against XPG (middle panel), or XPG null patient cells (XPCS2LV, lower panel), were irradiated with 2 Gy IR followed by 120 min repair and immunostaining using mouse anti-XPG (8H7) (red), and rabbit anti-53BP1 antibodies (green). The merged images for foci overlap (yellow), and DAPI (blue) stained nuclei are shown.
(E) Evidence for overlap of XPG foci with DSBs (53BP1 foci) is independent of the antibodies used (compare to panel D). hTERT immortalized HCA2 cells were mock treated (top) or treated with 2 Gy IR (bottom) and co-stained using rabbit anti-XPG (red) and mouse anti-53BP1 (green) antibodies, and DAPI (blue).

Figure S5. XPG interacts with HRR proteins; related to Figure 5.

(A) Interaction between XPG and RAD51. Co-immunoprecipitation of recombinant human XPG and RAD51 from Sf9 insect cells co-infected with baculoviruses expressing XPG and RAD51 was analyzed by western blotting.
(B) XPG forms stable trimers with HRR proteins. Insect cell cultures were co-infected with two baculoviruses expressing FLAG-BRCA2 and XPG, with the addition of a third baculovirus expressing either PALB2, DSS1, or RAD51. Trimeric complexes were purified by FLAG affinity chromatography and re-immunoprecipitated with XPG antibody or IgG control, followed by analysis by western blotting.
(C) Interaction between XPG and DSS1. Insect cells were co-infected with FLAG-XPG and DSS1, FLAG-BRCA2 and DSS1, or DSS1 alone, followed by FLAG affinity chromatography and analysis by western.

(D) XPG forms stable tetrameric complexes with HRR proteins. Insect cell cultures were co-infected with FLAG-BRCA2 and combinations of XPG, PALB2, DSS1, or RAD51 (as shown). Tetrameric complexes were purified by FLAG affinity chromatography, and then re-immunoprecipitated with IgG control and either RAD51 or PALB2 antibodies, followed by analysis by western blotting.

Figure S6. XPG promotes homologous recombination and chromatin binding of BRCA2, PALB2, and RAD51; related to Figure 6.

(A) XPG depletion impairs homologous recombination as assayed using a published integrated reporter construct (Nakanishi et al., 2005; Xia et al., 2006). The two-parameter dot plots display the FACS analysis from a representative experiment. The percentage of green fluorescent cells (FL1) is indicated at the lower right of each panel. FL1 (x-axis): green fluorescence from GFP+ cells; FL3 (y-axis): orange auto-fluorescence of all viable cells. The combined analysis of similar results from all experiments is shown in manuscript Figure 6A.

(B) Expression of recombinant I-SceI endonuclease in a representative gene conversion experiment (see Figure 6A and Figure S6A). DR-U2OS cells were transfected with the indicated siRNA and with an I-SceI expression plasmid expressing HA-tagged I-SceI, and then were processed by western analysis. QM, a transcription factor, was used as a loading control.

(C) Representative micrographs of RAD51 foci (green) after CPT treatment, with and without XPG depletion.

(D) Chromatin loading of HRR proteins in undamaged U2OS cells. U2OS cells were transfected with the indicated siRNAs, and then were treated with DMSO for 24 h, followed by western blotting of whole cell extracts, or of extracts fractionated into soluble (S100) or chromatin-bound (P100) proteins. Tubulin was a loading control for soluble proteins, and Histone H3 was a loading control for chromatin-bound proteins. Compare to results of similar analysis following CPT treatment in Figure 6.

(E) Quantification of PALB2 chromatin loading from Figure 6D and S6D. PALB2 signal for each P100 fraction was normalized to Histone H3 signal, and then normalized to the amount of chromatin-bound PALB2 in the control-depleted, CPT-damaged sample.

(F) Quantification of XPG chromatin loading from Figure 6D and S6D. XPG signal for each P100 fraction was normalized to Histone H3 signal, and then normalized to the amount of chromatin-bound XPG in the control-depleted, CPT-damaged sample.

Figure S7. XPG promotes single-strand annealing and BRCA1 function; related to Figure 7.

(A) Schematic of the reporter construct integrated into the SA-GFP cell line for measurement of single-strand annealing (SSA).

(B) Schematic of the reporter construct integrated into the EJ5-GFP cell line for measurement of total NHEJ events.

(C) XPG depletion does not affect total NHEJ. EJ5-GFP U2OS cells were transfected with the indicated siRNAs, followed by transfection with an I-SceI expression plasmid. The fraction of GFP positive cells was determined and normalized to the control siRNA transfected sample for each experiment. Data represent the mean ± SEM for N=6.

(D) XPG directly interacts with BRCA1. Extracts were generated from insect cells co-infected with baculovirus expressing human FLAG-tagged BRCA1 and/or untagged XPG. The proteins were co-purified by FLAG resin followed by SDS-PAGE and Coomassie stain.

(E) Whole cell extracts from U2OS cells transfected with siRNAs, treated with CPT (20 nM, 24 h), followed by CPT removal and harvest at the indicated times. Samples were examined by western for BRCA1, XPG, Tubulin, and Histone H3. (See Figure 7D for related analysis of these samples fractionated into soluble and chromatin-bound proteins).

(F) XPG protein increases in BRCA1 depleted cells. U2OS cells were transfected with the indicated siRNAs, and after 48 h, total cell extracts were analyzed for XPG and BRCA1, with tubulin as a loading control. Quantification of XPG protein with data showing the mean ± SEM for N=3.

(G) BRCA1 is hyperphosphorylated in XPG depleted cells. U2OS cells were transfected with the indicated siRNAs, and after 48 h were mock treated or treated with CPT (20 nM, 24 h), followed by 24 h recovery. The chromatin fraction (P100) was collected, and incubated with phosphatase buffer with or without lambda phosphatase (1 µl), and then analyzed for BRCA1 and Vimentin (loading control).

(H) Nuclear extracts (NE) were generated from U2OS cells that had been either mock treated with DMSO (0.1%) or treated with ATM inhibitor KU-55933 (10 μM) or ATR inhibitor VE822 (1 μM) for 16 h. Immunoprecipitations from the NE were performed with either control IgG (rabbit) or anti-XPG (rabbit). The amount of BRCA1 IP'd was normalized to the XPG IP'd in the same sample and plotted as shown. (I) 53BP1 foci (Figure 7F) were quantified and plotted. Data represent the mean ± SEM for N=3, with significance measured by Student's T test comparing untreated control KD with XPG KD (p=0.00179) or with BRCA1 KD (p=0.00422), or BRCA1 KD with XPG KD (p=0.02767). For the CPT treated samples, control KD was compared with XPG KD (p=0.006) or with BRCA1 KD (p=0.00011), versus comparing BRCA1 KD with XPG KD (p=0.02676).

Supplemental Experimental Procedures

Cell Culture

HCA2 foreskin fibroblasts were from J. Smith (University of Texas, USA). WI38 normal human fetal lung fibroblasts, VA13 (WI38, SV-40 transformed) fibroblasts, and XP-G/CS primary fibroblasts XPCS2LV (GM13370) and XP20BE (AG08803), were from Coriell (Camden, New Jersey). U20S and HeLa cells were from ATCC. DR-U2OS cells were from M. Jasin (Memorial Sloan-Kettering Cancer Center, USA) and SA-U2OS cells and EJ5-U2OS cells were from J. Stark (City of Hope, USA). SV-40 transformed fibroblast cells, XPCS1RO (XPG–deficient) were from S. Clarkson (University of Geneva), and XPCS1RO cells stably transfected with GFP, WT-XPG, or XPG-E791A were from O. Schärer (S.U.N.Y., Stony Brook). XPCS2LV fibroblasts were immortalized by infection with an hTERT expressing retrovirus as described for the HCA2 fibroblasts (Rubio et al., 2002). Cells were cultured under ambient oxygen levels and 10% CO_2 in DMEM supplemented with 10% fetal calf serum and 1% antibiotic/antimycotic. Primary mouse dermal fibroblasts from wt or *xpg*$^{-/-}$ mouse littermates (Barnhoorn et al., 2014) were cultured at 3% oxygen, 5% CO_2 in DMEM/Hams-F12 media supplemented with 20% fetal calf serum and 1% antibiotic/antimycotic.

Rationale for cell lines used in the study

Primary cells were used in initial experiments to interrogate XPG function. However, these cells are not amenable to biochemical studies due to their extremely slow growth rate. Therefore, U2OS cells were chosen because they are used commonly in the field of DNA damage signaling processes, they grow rapidly and have intact cell cycle check points, and the DR-GFP and SA-GFP cells used in this study were generated in this line. HeLa cells were used for chromosome aberration studies because they have a stable, although aneuploid karyotype. HCA2-hTERT fibroblasts were used for proliferation studies because they have active checkpoints in response to DNA damage. VA13 cells (SV-40 transformed, but WT XPG) were used as a comparison with the SV-40 transformed XP-G/CS cell line, XPCS1RO.

Small interfering RNA (siRNA) Transfection

Unless otherwise specified, siRNAs were ordered as annealed duplex RNA (Qiagen). siRNAs (40 nM) were transiently transfected into cells with Lipofectamine™RNAiMAX (Invitrogen) on two consecutive days, followed by re-plating, and incubation for 24-72 h prior to experimentation. XPG siRNAs were either transfected individually (40 nM) as specified in the text and figure legends, or were transfected as a mixture of siXPG-1 and siXPG-3 (20 nM each), noted as siXPG.

DNA target sequences:

Non-specific Control	5’-GATTCGAACGTGTCACGTCAA-3’
siXPG-1	5’-GGACTTAGCGTCCAGTGAC-3’
siXPG-2	5’-AGAATACATGCGGTGGATT-3’
siXPG-3	5’-GAAAGAAGATGCTAAACGT-3’
siXPC-2	5’-GCAAATGGCTTCTATCGAA-3’
siXPA-1	5’-GCTACTGGAGGCATGGCTA-3’
siPALB2-2	5’-CTTAGAAGAGGACCTTATTGT-3’
siBRCA1	5’-AAGGAACCTGTCTCCACAAAG-3’
siCtIP	5’-AAGCTAAAACAGGAACGAATC-3’

siRAD52 was from Silencer Pre-designed siRNA (AM16708, Ambion), and siRAD51AP1 was based on a previous publication (Wiese et al., 2007) and targets the RAD51AP1 ORF from 383-402.

Cell growth rate

To determine growth rate, cells were seeded at a subconfluent density of $4x10^4$ cells per 35 mm plate. At each time point, triplicate samples were harvested by trypsinization and quantified using a Coulter Counter. The cell number was plotted vs. time on a semi-log plot, and the doubling time was calculated from the linear portion of the graph. Comparisons of growth rates were performed with samples of similar age, as measured in passage doubling (PD). For example, normal cell lines WI38 (PD=28) and HCA2 (PD=32) were compared with XP-G/CS cell lines XPCS2LV (PD=26) and XP20BE (PD=28).

Cell-Cycle Analysis

Cells were trypsinized, collected by centrifugation, washed with PBS, fixed in ethanol, treated with RNase, stained with propidium iodide, and analyzed using a FACS Calibur (Becton-Dickinson). Cell cycle analysis was performed using FlowJo (Tree Star) and the Watson (pragmatic) algorithm.

Proliferation assay

hTERT-immortalized normal human fibroblast cells (HCA2-hTERT) were siRNA-depleted, re-plated, and 24 h later were treated as noted. Cells were then incubated in the presence of BrdU (20 μM) for 72 h, were harvested, washed with cold PBS and fixed and stored in ice-cold 70% ethanol. DNA was denatured with 2 M HCl, 0.5% Triton X-100 at room temperature with constant agitation for 1 h. Cells were incubated with fluorescein isothiocyanate (FITC)-conjugated anti-BrdU antibody (Becton Dickinson) for 1 h, and DNA was stained with propidium iodide in the presence of RNase. FACS to detect BrdU-positive cells was performed with a FACS Calibur (Becton-Dickinson), with analysis by FlowJo (Tree Star).

Micronuclei and Chromosome analysis

The cytokinesis-block micronucleus assay (Fenech et al., 2003) was used to score the formation of micronuclei (MN) in bi-nucleated cells as described earlier with minor modifications (Groesser et al., 2007). U2OS cells were treated with 3mg/ml Cytochalasin B immediately after treatment for 48 h. Cells were cytospun onto glass slides, coded and stained with 10 mg/ml acridine orange (Sigma) in PBS for 1 – 2 min. Following the scoring criteria described in detail (Fenech et al., 2003), 500 bi-nucleated cells in triplicates per treatment were analyzed using a Zeiss Axioskop microscope equipped with a 40x dry lens. Chromosome analysis was performed essentially as described with minor modifications (Wiese et al., 2007). HeLa cells were treated with colcemid (200 ng/ml; Sigma) for 6 h prior to harvest. Slides were coded prior to analysis of 50 metaphases per treatment using a Zeiss Axioskop 2 plus microscope equipped with a 100x oil lens. Gaps were counted as a chromatid breaks (ctb) when the gap size was wider than the chromatid.

Proteasome Inhibition.

U2OS cells treated with CPT were treated with the proteasome inhibitor MG132 (Calbiochem) at a concentration of 2 μM for 16 h prior to harvesting.

Whole Cell Extracts, Western Analysis, and Antibodies

For whole cell extracts, cells were lysed in SDS sample buffer (3% SDS, 10% glycerol, 100 mM Tris-HCl, pH 6.8) and heated at 95° C. For BRCA2, cell lysates were generated in the same buffer without heating, but with needle shearing. Protein concentrations were determined by the BCA assay (Pierce). Samples were mixed 1:1 with SDS sample buffer + 200 mM DTT + 0.5 mM bromophenol blue, prior to resolution on 4-12% Tris-Glycine, or 3-8% Tris-Acetate SDS-PAGE gels (Invitrogen), and were transferred to nitrocellulose membranes and probed with the corresponding antibodies. Antibodies used were mouse anti-XPG (8H7, Upstate), rabbit anti-XPG 97727, (Sarker et al., 2005), mouse anti-Ku80 (Hsu et al., 2002), rabbit anti-phospho RPA32 (Ser4/Ser8; A300-245A, Bethyl), mouse anti-RPA32 (Ab-3, Calbiochem), mouse anti-RAD51 (14B4, Sigma), rabbit anti-RAD51 (PC130, Oncogene), mouse

anti-BRCA2 (OP95, Calbiochem), mouse anti-BRCA1 (MABC199, Millipore), rabbit anti-PALB2 (A301-246A, Bethyl), rabbit anti-GST (G7781, Sigma), rabbit anti-XPA (sc853, Santa Cruz), rabbit anti-XPC (gift from A. Wani, The Ohio State University), mouse anti-tubulin (CP06, Calbiochem), rabbit anti-Histone H3 (ab1791, Abcam), mouse anti-p21 (F-5, Santa Cruz), and sheep anti-mouse (NA931V, GE Healthcare) and donkey anti-rabbit (NA934V, GE Healthcare) conjugated to horse radish peroxidase (HRP). Blots were imaged and quantified using a Versadoc 4000MP and Quantity One software (Biorad). Alternatively, proteins were detected by Western blot analysis using the Odyssey Infrared Imaging System (Li-Cor) using secondary antibodies Alexa Fluor 680 goat anti-mouse IgG (Invitrogen), or IRDye 800CW donkey anti-rabbit antibody (Li-Cor).

Cellular fractionation into soluble and chromatin-bound proteins

U2OS cells were trypsinized, washed with cold PBS, and fractionated as previously described (Xia et al., 2007; Xia et al., 2006) into S100 fraction containing cytoplasmic and nuclear proteins, and P100 fraction containing chromatin, nuclear matrix, and insoluble proteins. Briefly, the pellets were resuspended on ice in buffer containing 20 mM Tris pH 7.5, 1 mM EDTA, 0.5% NP-40, 100 mM NaCl and protease inhibitor cocktail for 10 min with gentle mixing, followed by centrifugation for 10 min at 14,000 rpm. The supernatant (S100 fraction) was removed, and the pellet (P100) was resuspended in an equal volume of SDS buffer with needle shearing. Fractionation quality was determined by immunoblotting for tubulin (S100-soluble) and for Histone H3 (P100-chromatin) proteins.

Lambda Protein Phosphatase treatment

U2OS cells were fractionated into the chromatin fraction (P100) and the pellets were resuspended in buffer containing 50 mM HEPES (pH 7.5), 100 mM NaCl, 2 mM DTT, 0.01% Brij 35, and 2 mM $MnCl_2$ with or without the addition of lambda phosphatase (1 µl) (NEB), and were incubated 30 min at 30^{o}C. SDS sample buffer was added followed by needle shearing. Samples were heated at 95^{o}C for 3 min and separated by SDS-PAGE and immunoblotted for BRCA1 and for Vimentin (loading control).

Nuclear extraction and immunoprecipitation

Nuclear extracts from U2OS cells were prepared as described (Dignam et al., 1983). Extracts (500-750 µg) were diluted to 140 mM NaCl prior to immunoprecipitation with magnetic Dynabeads Protein G (Invitrogen) pre-bound with antibody (4 µg). Beads were washed with the same buffer, followed by elution with SDS. Where noted, cells were treated with ATM inhibitor, KU55933 (VWR), ATR inhibitor, VE822 (Selleckchem), or the same concentration of DMSO for 16 h prior to harvest.

Indirect Immunofluorescence

When immunostaining for XPG, cells were grown in 4 or 8-well chamber slides (Invitrogen) either unsynchronized, or synchronized into G1 or S-phase as previously described (Davalos and Campisi, 2003). Cells were permeabilized with 0.5% Triton in CSK buffer (He et al., 1990) and fixed with 4% paraformaldehyde. Samples were blocked with 10% goat serum prior to incubating overnight at 4°C with primary antibodies including, polyclonal rabbit anti-XPG 97714 (Sarker et al., 2005), mouse anti-γH2AX (Ser139, clone JBW301, Millipore), mouse anti-53BP1 (MAB3802, Millipore), mouse anti-RAD51 (ab-2, Calbiochem), mouse anti-BRCA2 (clone 5.23, Millipore), and mouse anti-Cyclin A.

When immunostaining without XPG, cells were fixed with 4% para-formaldehyde and 0.3% Triton-X-100 in PBS prior to permeabilization with PBS containing 0.5% Triton X-100. Cells were blocked with 2% BSA, prior to addition of primary antibodies: rabbit anti-RAD51 (H-92, Santa Cruz), rabbit anti-53BP1 (Bethyl, A300-272A), and/or mouse anti-BRCA1 (MABC199, Millipore). Following PBS washes, samples were incubated with secondary antibodies conjugated to Alexa Fluors 488 or 594 (Molecular Probes) and with DAPI to stain nuclear DNA. Slides were mounted in Vectashield and viewed by epifluorescence. Images of cells were acquired on a microscope (BX60; Olympus) using a 40x UPlanFl 0.5 NA (Olympus) lens without oil and captured with a charge-coupled device camera (Diagnostic Instruments, Inc.) into SPOT imaging software (Diagnostic Instruments, Inc.). Alternatively, images were captured using a Zeiss Axiovert epifluorescence microscope with a Zeiss plan-apochromat 406 dry lens and a 12-bit charged coupled device camera (ORCA AG Hamamatsu). Images within the same data set were captured with the same exposure time, so that the intensities

were within the 12-bit linear range and could be compared between samples. Computer based image analysis to detect foci number was performed using BioSig Imaging Bioinformatics Platform (Parvin et al., 2007; Raman et al., 2007). All modifications were applied to the whole image using Photoshop CS2 (Adobe).

DNA fiber assay

Exponentially growing U2OS cells were transfected with the indicated siRNAs on two consecutive days, were replated, and on the following day (48 h post knockdown), were pulse labeled with 25 μM CldU (Sigma) followed by 250 μM IdU (Sigma) for 45 min each. For stalled replication forks, cells were pulse labeled with 25 μM CldU for 15 min, washed with PBS, incubated in 2mM HU for the times indicated, washed with PBS followed by a 250 μM IdU pulse label for 45 min. Labeled cells were harvested and DNA fiber spreads were prepared as described (Jackson and Pombo, 1998). Acid treated fiber spreads were stained with monoclonal rat anti-BrdU (Oxford Biotechnologies, 1:1000) followed by monoclonal mouse anti-BrdU (Becton Dickinson, 1:1500). Secondary antibodies were goat anti-rat AlexaFluor 555 and goat anti-mouse AlexaFluor 488 (1:500, Invitrogen). Fibers were examined using fluorescence microscopy using an Axiovert 119 (Zeiss, Germany). CldU and IdU tracts were measured using ImageJ and values were converted into kilobases (Jackson and Pombo, 1998). At least 200 forks were analyzed. Different classes of tracts were classified; red-green (elongating fork), red (stalled or terminated forks), green-red-red-green (1st pulse origin) and green (2nd pulse origin). Frequencies were calculated using ImageJ. Statistical analysis and graphs were performed by means of the computer program Prism (GraphPad Software, San Diego, USA). Data are given as mean (± SEM) of replicate experiments.

Quantitative Real-Time Polymerase Chain Reaction (qRT-PCR)

RNA was purified using Qiagen RNeasy® Kit. cDNA was constructed from purified RNA using a High-Capacity cDNA Reverse Transcription Kit (Applied Biosystems). Target transcripts were amplified using TaqMan® Fast Universal PCR Mix (Applied Biosystems) and Taqman® primers (XPG:

Hs00164482_m1; β-Actin: Hs99999903_m1) on an Applied Biosystems® 7500 Real-Time PCR System. β-Actin was used as the endogenous control in experiments. Expression levels of untreated control cells were used for calibration. Fold-change (FC) was calculated from the following [15]:

$$\Delta CT = avg\ CT_{target} - avg\ CT_{endogenous\ control}$$

$$\Delta\Delta CT = \Delta CT_{target} - \Delta CT_{calibrator}$$

$$FC = 2^{(-\Delta\Delta CT)}$$

$$stdev_{\Delta\Delta CT} = stdev_{\Delta CT} = \sqrt{(stdev_{endogenous\ control})^2 + (stedev_{target})^2}$$

$$stdev_{FC} = (\ln 2)(stdev_{\Delta\Delta CT})(2^{(-\Delta\Delta CT)})$$

Gene conversion and single-strand annealing assays

DR-U2OS cells (Nakanishi et al., 2005; Xia et al., 2006) were seeded, and transfected 24 h later with siRNA (40 nM) and Lipofectamine RNAiMax (Invitrogen) in OPTI-MEM medium. Cells were re-transfected 24 hr later with 40 nM siRNA and 0.8 µg I-SceI-encoding plasmid with Lipofectamine2000 (Invitrogen). SA-U2OS cells were seeded and transfected as described (Gunn and Stark, 2012). Flow cytometry was carried out 72 h after the second transfection to measure GFP positive cells.

Insect cell co-expression and co-immunoprecipitation

Recombinant human XPG (untagged) and GST-PALB2 baculoviruses were produced as described previously (Dray et al., 2010; Sarker et al., 2005). The 6xHis-BRCA2-FLAG and GST-DSS1 expression vectors were produced as described (Zhao et al., 2015). The pFastBac 1/FLAG-BRCA1 vector was originally provided by the lab of Jeffrey Parvin (The Ohio State University). The baculovirus transfer vectors for RAD51 and XPG-FLAG were constructed by subcloning a PCR amplified DNA fragment containing the full-length RAD51 or the full-length XPG with a C-terminal FLAG tag into pFastBac 1. The recombinant baculoviruses for 6xHis-BRCA2-FLAG, RAD51, FLAG-BRCA1, and XPG-FLAG were generated in Sf9 insect cells using a Bac-to-Bac protocol (Invitrogen). Proteins were expressed in High Five insect cells by infecting with baculoviruses expressing 6xHis-BRCA2-FLAG, XPG, XPG-FLAG,

GST-PALB2, GST-DSS1, RAD51, and FLAG-BRCA1, as denoted for 40 h. For FLAG affinity pull-downs, cell pellets (100 ml cultures) were resuspended in 6 ml of lysis buffer (50 mM Tris. HCl, pH 7.4, 150 mM NaCl, 1 mM $MgCl_2$, 1 mM beta-mercaptoethanol, and 0.5% NP-40) supplemented with 1 mM PMSF, protease inhibitor cocktail (Roche), and 1 µl benzonase per 10^7 cells (Sigma), and lysed by Dounce homogenization (40 strokes). After incubation on ice for 45 min, the lysate was clarified by centrifugation at 12,000xg for 30 min at 4^{o}C. The supernatant was incubated with 50 µL of FLAG-M2 agarose beads (Sigma) at 4^{o}C for 1.5 h, washed with 20 ml of lysis buffer, and eluted three times with 50 µl of 200 µg/ml 3xFLAG peptide (Sigma), each with 15 min incubation on ice. For co-immunoprecipitations, antibodies (4 µg) were bound to Dynabeads Protein G (Invitrogen) at 4^{o}C for 1 h. The FLAG elutions were pooled, split into two parts, incubated overnight at 4^{o}C with antibody-bound beads, followed by extensive wash (5 times with 0.5 ml of lysis buffer) and elution in 50 µl of 5x ImmunoPure Lane Marker reducing sample buffer (Pierce) for 10 min at room temperature.

SUPPLEMENTAL REFERENCES

Barnhoorn, S., Uittenboogaard, L.M., Jaarsma, D., Vermeij, W.P., Tresini, M., Weymaere, M., Menoni, H., Brandt, R.M., de Waard, M.C., Botter, S.M.*, et al.* (2014). Cell-autonomous progeroid changes in conditional mouse models for repair endonuclease XPG deficiency. PLoS Genet *10*, e1004686.

Davalos, A.R., and Campisi, J. (2003). Bloom syndrome cells undergo p53-dependent apoptosis and delayed assembly of BRCA1 and NBS1 repair complexes at stalled replication forks. J Cell Biol *162*, 1197-1209.

Dignam, J.D., Lebovitz, R.M., and Roeder, R.G. (1983). Accurate transcription initiation by RNA polymerase II in a soluble extract from isolated mammalian nuclei. Nucleic Acids Res *11*, 1475-1489.

Dray, E., Etchin, J., Wiese, C., Saro, D., Williams, G.J., Hammel, M., Yu, X., Galkin, V.E., Liu, D., Tsai, M.S.*, et al.* (2010). Enhancement of RAD51 recombinase activity by the tumor suppressor PALB2. Nat Struct Mol Biol *17*, 1255-1259.

Fenech, M., Chang, W.P., Kirsch-Volders, M., Holland, N., Bonassi, S., and Zeiger, E. (2003). HUMN project: detailed description of the scoring criteria for the cytokinesis-block micronucleus assay using isolated human lymphocyte cultures. Mutat Res *534*, 65-75.

Groesser, T., Chun, E., and Rydberg, B. (2007). Relative biological effectiveness of high-energy iron ions for micronucleus formation at low doses. Radiat Res *168*, 675-682.

Gunn, A., and Stark, J.M. (2012). I-SceI-based assays to examine distinct repair outcomes of mammalian chromosomal double strand breaks. Methods Mol Biol *920*, 379-391.

He, D.C., Nickerson, J.A., and Penman, S. (1990). Core filaments of the nuclear matrix. J Cell Biol *110*, 569-580.

Hsu, H.L., Yannone, S.M., and Chen, D.J. (2002). Defining interactions between DNA-PK and ligase IV/XRCC4. DNA Repair (Amst) *1*, 225-235.

Jackson, D.A., and Pombo, A. (1998). Replicon clusters are stable units of chromosome structure: evidence that nuclear organization contributes to the efficient activation and propagation of S phase in human cells. J Cell Biol *140*, 1285-1295.

Mazroui, R., Di Marco, S., Kaufman, R.J., and Gallouzi, I.E. (2007). Inhibition of the ubiquitin-proteasome system induces stress granule formation. Mol Biol Cell *18*, 2603-2618.

Nakanishi, K., Yang, Y.G., Pierce, A.J., Taniguchi, T., Digweed, M., D'Andrea, A.D., Wang, Z.Q., and Jasin, M. (2005). Human Fanconi anemia monoubiquitination pathway promotes homologous DNA repair. Proc Natl Acad Sci U S A *102*, 1110-1115.

Parvin, B., Yang, Q., Han, J., Chang, H., Rydberg, B., and Barcellos-Hoff, M.H. (2007). Iterative voting for inference of structural saliency and characterization of subcellular events. IEEE Trans Image Process *16*, 615-623.

Raman, S., Maxwell, C.A., Barcellos-Hoff, M.H., and Parvin, B. (2007). Geometric approach to segmentation and protein localization in cell culture assays. Journal of microscopy *225*, 22-30.

Rubio, M.A., Kim, S.H., and Campisi, J. (2002). Reversible manipulation of telomerase expression and telomere length. Implications for the ionizing radiation response and replicative senescence of human cells. J Biol Chem *277*, 28609-28617.

Sarker, A.H., Tsutakawa, S.E., Kostek, S., Ng, C., Shin, D.S., Peris, M., Campeau, E., Tainer, J.A., Nogales, E., and Cooper, P.K. (2005). Recognition of RNA polymerase II and transcription bubbles by XPG, CSB, and TFIIH: insights for transcription-coupled repair and Cockayne Syndrome. Mol Cell *20*, 187-198.

Staresincic, L., Fagbemi, A.F., Enzlin, J.H., Gourdin, A.M., Wijgers, N., Dunand-Sauthier, I., Giglia-Mari, G., Clarkson, S.G., Vermeulen, W., and Scharer, O.D. (2009). Coordination of dual incision and repair synthesis in human nucleotide excision repair. EMBO J *28*, 1111-1120.

Wiese, C., Dray, E., Groesser, T., San Filippo, J., Shi, I., Collins, D.W., Tsai, M.S., Williams, G.J., Rydberg, B., Sung, P.*, et al.* (2007). Promotion of homologous recombination and genomic stability by RAD51AP1 via RAD51 recombinase enhancement. Mol Cell *28*, 482-490.

Xia, B., Dorsman, J.C., Ameziane, N., de Vries, Y., Rooimans, M.A., Sheng, Q., Pals, G., Errami, A., Gluckman, E., Llera, J.*, et al.* (2007). Fanconi anemia is associated with a defect in the BRCA2 partner PALB2. Nat Genet *39*, 159-161.

Xia, B., Sheng, Q., Nakanishi, K., Ohashi, A., Wu, J., Christ, N., Liu, X., Jasin, M., Couch, F.J., and Livingston, D.M. (2006). Control of BRCA2 cellular and clinical functions by a nuclear partner, PALB2. Mol Cell *22*, 719-729.

Zhao, W., Vaithiyalingam, S., San Filippo, J., Maranon, D.G., Jimenez-Sainz, J., Fontenay, G.V., Kwon, Y., Leung, S.G., Lu, L., Jensen, R.B.*, et al.* (2015). Promotion of BRCA2-Dependent Homologous Recombination by DSS1 via RPA Targeting and DNA Mimicry. Mol Cell *59*, 176-187.